

# Efficient Edge Detection Using Fuzzy Heuristic Particle Swarm Optimization

Noor Elaiza Abdul Khalid<sup>1,4</sup>, Mazani Manaf<sup>2</sup> and Mohd Ezane Aziz<sup>3</sup>

<sup>1,2</sup>Faculty of Computer and Mathematical Sciences  
Universiti Teknologi MARA (UiTM), Malaysia

<sup>3</sup>Radiology Department  
Hospital USM, Kubang Kerian  
Universiti Sains Malaysia, Kelantan, Malaysia

<sup>4</sup>Email: elaiza@tmsk.uitm.edu.my

## ABSTRACT

*This paper presents a hybridization of Particle Swarm Optimization (PSO) and Fuzzy edge detector. The edge detector is used as the initial population and as the objective function. The purpose of hybridizing the algorithm is to create an optimized edge detector. Classical Fuzzy Heuristics (CFH) detects thick edges. These thick edges need to be optimized to obtain a thin line. In this research the PSO is used to optimize the edge detection detected by the CFH algorithm and it is referred to as FHPSO. The test images are radiographs images of the metacarpal. These images have been used, because there is a need to detect strong and thin edges. Radiograph images are noisy in nature, which makes it difficult to measure the cortical thickness, the cortical outline of the inner cortical and outer cortical of the long tubular bone. The outer cortical edges are considered to be the strong edges due to high discontinuity values and the inner cortical edges are considered weak edges due to low their discontinuity values. The performance of FHPSO in detecting edges has been shown to be quite efficient.*

**Keywords:** Fuzzy heuristics, Particle swarm optimization, tubular bone, Radiographs

## Introduction

Medical image computing has revolutionized the field of medicine by providing novel methods to extract and visualize information from medical data. These data maybe acquired using various acquisition modalities. The eye is the most complex part of human vision. Simulation and interpreting images is the most challenging and complex part in computer visualization. Image segmentation in medical images is a very complex task. Medical images are difficult to segment due to the fact that they contain grainy image regions and overlapping of anatomical features [1]. The anatomy that is of interest may not be separable from its surroundings due to gray level inconsistency and the lack of strong edges at its border. Radiographic digital imaging is used for various procedures in many medical disciplines particularly examining bone tissue. However, radiographs may be of low contrast, contain blurred edges, faint details due to scattering, radiation and body structure complexities [2, 3].

*Fuzzy techniques* in edge detection have become more imperative in digital image processing. An edge can be defined as the boundary between two regions separated by two relatively distinct gray-level properties [4]. The process of edge detection reduces an image to its edge details, which yields the outline of an object that is often used for feature extraction and object recognition. Recent researchers have implemented and exploited fuzzy techniques are [5-8]. Tizhoosh introduced a heuristic membership function, simple fuzzy rules and fuzzy complements in his edge detector system [9]. Hirota employed both triangular and Gaussian membership functions in image compression [10]. See *et al.* [11] used modified Gaussian membership functions.

The *particle swarm paradigm* is a new algorithm implemented in heuristic optimization. In the last few years, Particle Swarm Optimization (PSO) has been used to solve many optimization problems. PSO is a bio-inspired stochastic optimization population-based evolutionary computation technique [12]. It is a simple concept based on the characteristics of the nature of swarm behavior and is what makes PSO easy to implement. This has attributed to its rapid development and application in many different fields [13-17].

This paper presents a *Fuzzy Particle Swarm Optimization (FHPSO)* edge detector. FHPSO incorporates a fuzzy heuristics edge detection membership function as part of the objective function. This technique also uses the fuzzy heuristics edge detection algorithm as the initial

population for the PSO algorithm. The fuzzy heuristic edge detector is called Classical Fuzzy Heuristics (CFH). The main challenge for this algorithm is to detect the outer cortical (OC) and inner cortical (IC) of a bone. The OC is considered to yield strong edges due to distinctly higher gray level changes between the cortical area, which is light gray and the background, which is essentially black. The IC is considered to yield weak edges, because of lower gray level variation between the trabeculae area, which is gray in color, and the cortical area, which is a lighter gray. The position of the OC and IC edges that are detected are used to measure the cortical thickness (CT). These measurements are in turn used to calculate the inner diameter (ID) and the outer diameter (OD) of the cortical. This research focuses on obtaining the cortical outline of the diaphyseal area of the metacarpal.

## **Approach and Methods**

Radiographic images typically suffer from low resolution, high levels of noise, low contrast, geometric deformation and the presence of artifacts [1]. Seventy computed hand radiographs have been used in this research. The radiographs used in this research are of the non-dominant hand. The images are retrospective images acquired as secondary data from the Hospital Universiti Sains Malaysia (HUSM) [18]. An image pre-processing method has been used to extract three metacarpals from the hand radiographs. Only metacarpals C2, C3 and C4 are used in this study, because metacarpals C1 and C5 have short diaphyseal areas.

Digital methods are used in medical diagnosis to get better results and elucidate more information. There are several methods used in digital medical diagnosis, in general the methodology consists of three phases, which are the preprocessing phase where smoothing filters are used to reduce noise, followed by fuzzy edge detection and finally optimization. As discussed in previous research [3], radiograph images are often fuzzy and noisy. The preprocessing stage uses median  $5 \times 5$  as smoothing filters, which smoothens images without blurring the edges.

The implementation of the fuzzy heuristic edge detection algorithm [19] is used to identify the search space. This stage can significantly reduce the search space and thus also perhaps reduces the speed of processing.

### Classical Fuzzy Heuristics (CFH)

The spatial domain image of the phantom hand image is represented in the fuzzy domain. The  $M \times N$  dimensional image and  $L$  levels can be taken as an array of fuzzy singleton sets. The edges are detected according to equation 1:

$$X = \{(\mu_{mn}, x_{mn}); m = 1, 2, \dots, M; n = 1, 2, \dots, N; 0 \leq \mu \leq 1\}$$

$x_{mn}$  = gray scale level of brightness

$$X = \bigcup_{m=1}^M \bigcup_{n=1}^N \frac{\mu_{mn}}{g_{mn}} \quad (1)$$

The membership function  $\mu_{mn}$  is obtained according to equation 2:

$$\mu_{mn} = \frac{g_{mn}}{\max_{i \in \{1, M\}, j \in \{1, N\}} g_{i,j}} \quad (2)$$

The image  $X'$  containing all edges is calculated according to equation 3:

$$X' = \bigcup_{m=1}^M \bigcup_{n=1}^N \frac{\hat{\mu}_{mn}}{g_{mn}} \quad (3)$$

where

$$\mu_{mn} = \text{degree of edginess}$$

$$g_{mn} = \text{center of pixel}$$

The membership is based on the gray level difference of the center pixel, value  $g_{mn}$ , and the surrounding neighboring pixels within a window of size  $W \times W$  as show in equation 4 [9]:

$$\hat{\mu}_{mn} = \frac{\sum_i \sum_j |g_{ij} - g_{mn}|}{\Delta + \sum_i \sum_j |g_{ij} - g_{mn}|} \quad (4)$$

The lower the  $\Delta$  values, the more edges are detected. The advantage of defining the degree of edginess as a fuzzy membership function is that the entire fuzzy set theory can be further modified. The results from CFH are used as the search space to be optimized by the FPSO. CFH selects the bone edges and significantly removes background noise, thus reducing the search space area [19]. Further noise reduction is done by preprocessing the images with mean  $5 \times 5$  smoothing filters.

## **Particle Swarm Optimization**

In 1995, Kennedy and Eberhart designed an algorithm inspired by social interactions of individuals within a swarm, for example a flock of birds, a school of fish, or even humans. This algorithm is a population based stochastic optimization technique named Particle Swarm Optimization (PSO) [12]. PSO is a population-based search process where individual particles are grouped into a swarm. Each particle in the swarm represents a probable and potential optimized candidate solution. In a PSO system, each particle is “flown” through the multidimensional search space, adjusting its position in the search space according to its social and cognitive interaction between itself and its neighbours. It will reposition itself towards an optimum solution (pbest). A global best solution is discovered among the pbest outcomes [20]. Therefore, if a particle finds a new potential solution, all other particles will move closer to it, thus requiring a thorough exploration of the solution space.

PSO consists of two main components, namely the cognitive and the social components. The *cognitive component* quantifies the performance of particle  $i$  relative to past performances or resembles individual memory of the position that was best for the particle. The effect of this term is that particles are drawn back to their own best positions, resembling the tendency of individuals to return to situations or places that satisfied them the most in the past [21].

In an early analysis, Kennedy provided empirical evidence that the *social-only* model is faster and more efficient than the *full* and *cognitive-only* models [22]. These models were defined by omitting components of the *velocity formula*. The complete model is a combination of the cognitive component and the social components. Dropping the social component results in the *cognition-only* model, whereas dropping the cognition component defines the *social-only* model. In a fourth model, the *selfless* model, the neighbourhood best is chosen only from the neighbours, without considering the current individual. Carlisle and Dozier tested these four models in dynamic changing environments [23]. They empirically proved that the *social-only* model consistently found solutions faster than the *full* model. This research focuses more on the social components where the chosen particle is the best particle in a particular local neighbourhood.

## The Fuzzy Particle Swarm Optimization Algorithm (FPSO)

The FPSO consists of four main steps: the population selection, the objective function, the velocity or position, and the stopping function. However the implementation of PSO poses two distinct and tricky challenges; determine the population selection method and the objective function. PSO is a method for optimization. As discussed in the previous section, fuzzy edge detection is used to find the initial edges of the IC and the OC. These edges are thick and makes it difficult to measure the Cortical Thickness (CT), the internal diameter (ID) and the outer diameter (OD) of the metacarpal. Thus these edge pixels are chosen as the initial swarm population or search space.

PSO consists of several parameters that play an important role in determining the success rate of any evolutionary algorithm. In this research only two parameters have been considered, namely the swarm size [24] and neighbourhood size [25]. The approach adopted in this research generally uses a swarm size of  $n =$  Number of selected particles from the fuzzy edge detector and a neighbourhood size of  $k = 3 \times 3$ . The objective function is based on the fuzzy heuristics membership function with a  $3 \times 7$  neighbourhood that acts as noise eliminator.

FPSO also consists of four steps, namely dynamic population selection, the edge test or the velocity to determine the *lbest* pixels, the connectivity test or the objective function to determine the final IC or OC edges, which is the *gbest* pixels, and the stopping function. This research has tried to solve the population selection method by using the fuzzy edge detection algorithm as the objective function. The fittest particle is determined by selecting the pixels that have the highest membership value, *lbest*. The selected pixel must also be connected to other pixels that have been selected as the previous *lbest*. A flowchart of the PSO algorithm is presented in Figure 1.

The four FPSO steps are described in greater detail as follows:

### Step 1: Dynamic Population Selection

The CFH algorithm is used to perform the initial particle selection. The threshold level in determining the membership of the edge pixels to be selected is set at 0.2 [19]. This threshold level has the advantage of the highest connectivity and the maximizing the number of IC and OC edge pixels detected. The large number of pixels ensures that all the true edges are considered as possible solutions.

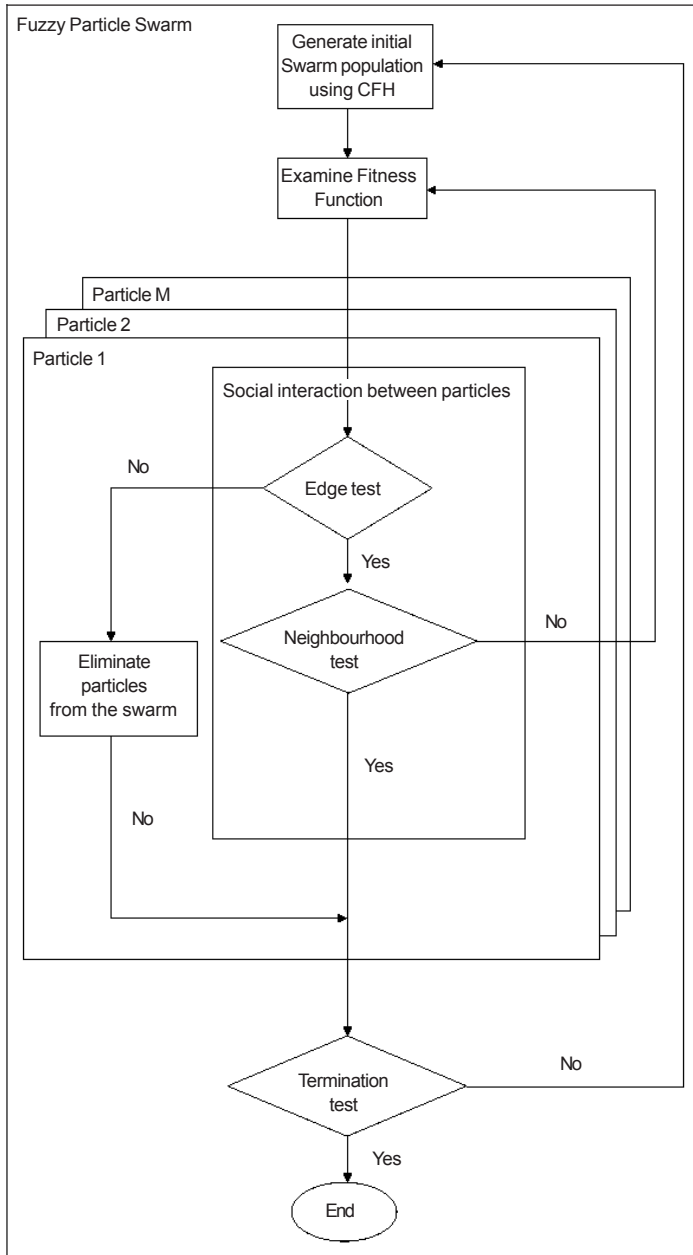


Figure 1: Proposed Fuzzy Particle Swarm Optimization (FPSO) Edge Detection Process

**Step 2:** Edge test or the velocity to determine the *lbest* pixels

The algorithm starts by scanning from the leftmost selected edge pixel population  $P_{xy}$ . Then the pixel at the membership value of the top neighboring pixel  $P_{x'y'}$  is tested against the pixels  $P_{x1y1}$ ,  $P_{x2y2}$  and  $P_{x3y3}$  as in Figure 2.  $P_{x'y'}$  will be considered as the new selected edge position or *lbest* in the neighborhood if its fuzzy membership value is greater than the values of all the tested pixels. This selected pixel can then replace the  $P_{xy}$  as center of the neighborhood and the process is iterated ten times.

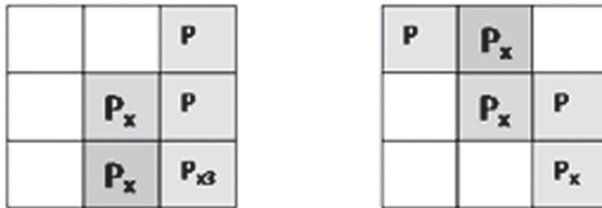


Figure 2: Edge Test Pixels in  $3 \times 3$  Neighborhood

**Step 3:** The connectivity test or the objective function to determine the final IC or OC edges which is the *Gbest* pixels

The purpose of this test is to eliminate noise and to test that the pixels under consideration have more than five other neighboring pixels that are also considered as edges. To conduct the connectivity test a neighborhood of  $3 \times 8$  is counted for the selected *lbest* pixels, as shown in Figure 3. The *lbest* pixels will be considered as the *gbest* if more than 5 of the pixels are selected as *lbest*.

**Step 4:** Stopping function

The iteration will only end when all the selected edge population pixels have been processed.

**Results and Discussion**

The results will be discussed with respect to the visual performance and a quantitative comparison between the cortical measurements obtained



x- -	x, y -	x+ -
x- -	x, y -	x+ -
x- -	x, y -	x+ -
x- -	x, y -	x+ -
x- -	x, y -	x+ -
x- -	x, y -	x+ -
x- -	x, y -	x+ -

Figure 3: The Neighborhood Connectivity Test

from the FPSO and manual measurements made with micro calipers performed by a radiologist [18].

### **Visual Performance of the FPSO**

Samples of images processed with the various FPSO techniques proposed in the research are presented in Figure 4. Visually it can be seen that the FPSO has been successful in finding a thin edge for the IC and OC. The result of implementing this algorithm can be observed in Figure 4.

Even though the outline of the image is clear it is evident that not all the OC and IC edges are detected. The C2 edges in Figure 4 still contain a degree of noise, which is evident from the disconnected lines. To quantify this region of interest (ROI) composed of eighty lines, a scan is performed to detect the number of complete IC and OC edges. Each line scan must detect four edge pixels that is the left OC (LOC), left IC (LIC), right IC (RIC) and the right OC (ROC). The summary of the results is tabulated in Table 1. C2 has 95 % completed line edges, 97.5 % 83.75 % for C3 and C4, respectively, Table 1.

FHPSO managed to detect a high percentage of complete edges. The standard deviations are rather high among the different images and these discrepancies may be attributed to the nature of the radiographs image intensities during the acquirement process.

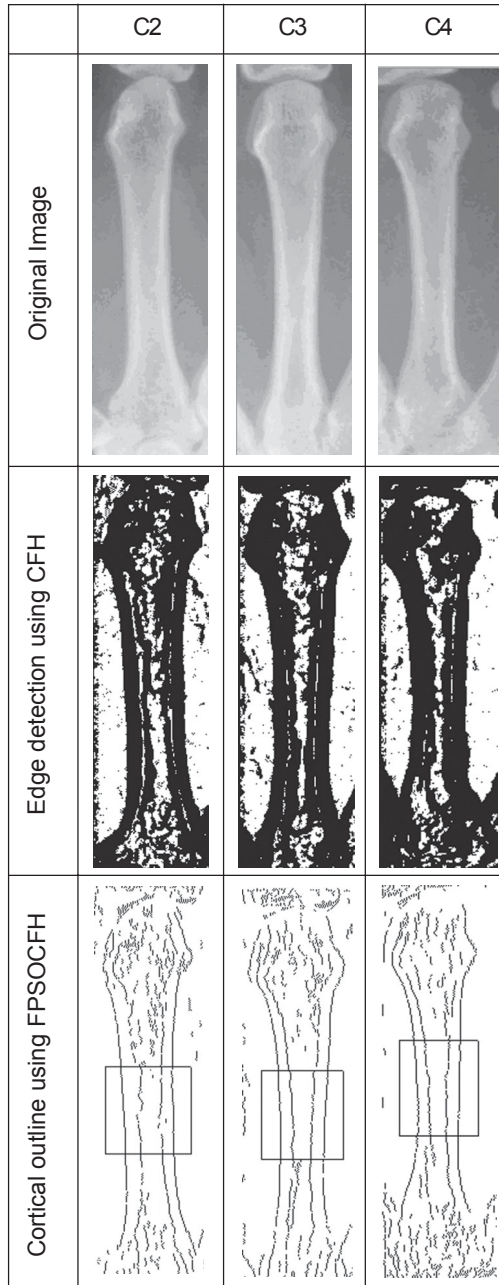


Figure 4: Sample of Visual Comparison of Using, FPSOCFH

Table 1: Summary of the Number of Complete LP, LE, RE and RP Edges Detected Using the Various FHPSO for 130 Images

	Mean	SD of the Mean	Percentage
C2	76	9.96	95
C3	78	16.62	97.5
C4	67	24.22	83.75

### Results of the Geometric Measurements

This section discusses the geometric measurements and how the measurements made by the FPSO correlate with the manual measurements. This comparison will determine the accuracy of the FSPO edge detection method. Table 2 presents a summary of the measurements of the left cortical width, right cortical width, internal diameter (ID) and outer diameter (OD) grouped according to the different age groups for metacarpal C2. As expected the cortical thickness (CT) reduces with age for all metacarpals measured. The standard deviation measurements are low, which indicates the accuracy of the measurements.

Table 2: Results Obtained from FPSO Edge Detection Method for Metacarpal C2

		C2				
		LCW (mm)	RCW (mm)	ID (mm)	OD (mm)	CT (mm)
20-29	MN	2.06	2.31	2.82	7.19	4.37
	SD	±0.21	±0.19	±0.68	±0.78	±0.38
30-39	MN	1.98	2.24	2.24	6.46	4.22
	SD	±0.19	±0.26	±0.63	±0.46	±0.36
40-49	MN	2.00	2.15	2.5	6.65	4.15
	SD	±0.27	±0.63	±0.61	±0.41	±0.07
50-59	MN	2.02	2.16	2.47	6.66	4.18
	SD	±0.14	±0.27	±0.54	±0.53	±0.24
60-69	MN	1.67	1.83	2.57	6.07	3.5
	SD	±0.2	±0.12	±0.35	±0.44	±0.31
70-79	MEAN	1.91	1.77	4.1	7.78	3.68
	SD	±0.28	±0.33	±1.22	±0.74	±0.58

Table 3 presents a summary of the measurements of the left cortical width (LCW), right cortical width (RCW), internal diameter (ID) and outer diameter (OD) grouped according to the different age groups for metacarpal C3. The trend in the cortical thickness (CT) reduces with age for the metacarpals measured. The standard deviation measurements are again low.

Table 3: Results Obtained from FPSO Edge Detection Method for Metacarpal C3

		C3				
		LCW (mm)	RCW (mm)	ID (mm)	OD (mm)	CT (mm)
20-29	MN	1.99	2.03	2.94	6.96	4.02
	SD	±0.29	±0.37	±0.82	±0.82	±0.63
30-39	MN	1.99	2.01	2.46	6.46	4
	SD	±0.15	±0.2	±0.81	±0.73	±0.28
40-49	MN	1.86	1.89	2.74	6.5	3.76
	SD	±0.23	±0.75	±0.5	±0.45	±0.09
50-59	MN	1.91	1.96	2.35	6.22	3.87
	SD	±0.22	±0.18	±0.49	±0.51	±0.34
60-69	MN	1.58	1.7	2.76	6.04	3.28
	SD	±0.15	±0.22	±0.23	±0.51	±0.33
	MEAN	1.6	1.49	3.76	6.85	3.09
70-79	SD	±0.12	±0.42	±0.8	±0.5	±0.53

Table 4 presents the summary of the measurements of the left cortical width, right cortical width, internal diameter (ID) and outer diameter (OD) grouped in to the different age group for Metacarpal C4. The cortical thickness (CT) trend is similar to that for Metacarpal C2 and C3.

The results of the measurement of the LCW, RWC, ID, OD and CT are larger for C2, slightly smaller for C3 and are the smallest for C4. The small standard deviation in all the tables indicates accuracy within the measurements. This is further corroborated by comparison with the average ID and OD manual measurements presented in Table 5.

It is observed that there is little difference between the ID and OD values for the FPSO and manual measurements, however the standard deviations for the manual measurements are higher than those for the FPSO method.

Table 4: Results Obtained from FPSO Edge Detection Method for Metacarpal C4

		C4				
		LCW (mm)	RCW (mm)	ID (mm)	OD (mm)	CT (mm)
20-29	MN	1.71	1.7	2.07	5.48	3.41
	SD	±0.22	±0.26	±0.68	±0.87	±0.48
30-39	MN	1.63	1.6	1.93	5.16	3.23
	SD	±0.19	±0.28	±0.66	±0.45	±0.45
40-49	MN	1.53	1.52	2.19	5.25	3.05
	SD	±0.25	±0.65	±0.59	±0.4	±0.1
50-59	MN	1.54	1.52	2	5.06	3.06
	SD	±0.15	±0.16	±0.51	±0.48	±0.26
60-69	MN	1.45	1.37	2.07	4.88	2.82
	SD	±0.18	±0.17	±0.41	±0.3	±0.34
70-79	MEAN	1.44	1.34	2.72	5.49	2.77
	SD	±0.22	±0.2	±0.72	±0.34	±0.41

Table 5: Comparison of the ID and OD Measurements from FPSOCFH with Manual Measurements for C2

		ID(mm)		OD(mm)	
		MAN	FPSO	MAN	FPSO
20-29	MEAN	3.12	2.82	7.49	7.19
	SD	±0.85	±0.68	±0.63	±0.78
30-39	MEAN	2.67	2.24	7.46	6.46
	SD	±0.68	±0.63	±0.51	±0.46
40-49	MEAN	2.71	2.5	7.47	6.65
	SD	±0.74	±0.61	±0.63	±0.41
50-59	MEAN	2.31	2.47	7.39	6.66
	SD	±0.63	±0.54	±0.6	±0.53
60-69	MEAN	3.11	2.57	7.43	6.07
	SD	±0.59	±0.35	±0.84	±0.44
70-79	MEAN	4.2	4.1	8.23	7.78
	SD	±1.23	±1.22	±0.63	±0.74

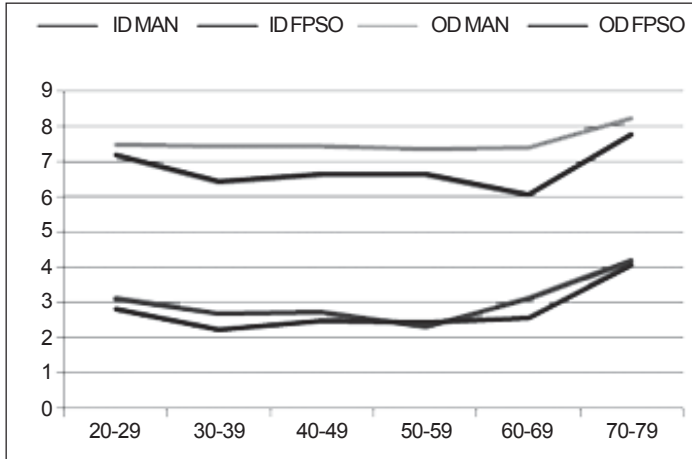


Figure 5: Line graph of the ID and OD Measurements for the FPSO and Manual Measurement for C2

The trends for both sets of measurements are essentially the same, Figure 5. Table 6 presents the comparison between ID and OD measurements for metacarpal C3. The measurements for C3 are very similar to the measurements for C2, furthermore the C3 and C2 ID and OD standard deviations are also low.

Table 6: Comparison of the ID and OD Measurements from FPSOCFH with Manual Measurements for C3

		ID(mm)		OD(mm)	
		MAN	FPSO	MAN	FPSO
20-29	MEAN	3.01	2.94	7.04	6.96
	SD	±0.79	±0.82	±0.57	±0.82
30-39	MEAN	2.63	2.46	7.08	6.46
	SD	±0.7	±0.81	±0.61	±0.73
40-49	MEAN	2.81	2.74	7.16	6.5
	SD	±0.88	±0.5	±0.55	±0.45
50-59	MEAN	2.41	2.35	6.92	6.22
	SD	±0.66	±0.49	±0.54	±0.51
60-69	MEAN	3.13	2.76	6.93	6.04
	SD	±0.15	±0.23	±0.69	±0.51
70-79	MEAN	3.91	3.76	7.21	6.85
	SD	±0.93	±0.8	±0.4	±0.5

The line trend for the C3 ID measurements are very similar, Figure 6. However the OD measurements differ by almost 1 mm.

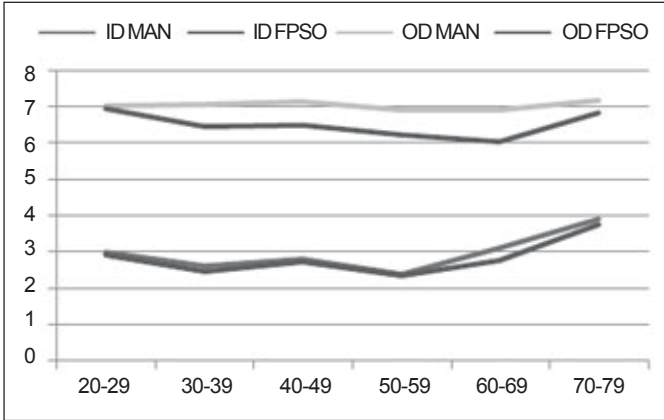


Figure 6: Line Graph of the ID and OD Measurements for The FPSO and Manual Measurement for C3

The results of the ID and OD measurements for C4 are almost similar to the C2 and C3 measurements. The C4 measurement standard deviations are also low, Table 7.

Table 7: Comparison of the ID and OD Measurements from FPSO with Manual Measurements for C4

		ID		OD	
		MAN	FPSO	MAN	FPSO
20-29	MEAN	2.53	2.07	5.84	5.48
	SD	±0.72	±0.68	±0.58	±0.87
30-39	MEAN	2.09	1.93	5.77	5.16
	SD	±0.71	±0.66	±0.55	±0.45
40-49	MEAN	2.14	2.19	5.73	5.25
	SD	±0.78	±0.59	±0.58	±0.4
50-59	MEAN	1.89	2	5.69	5.06
	SD	±0.62	±0.51	±0.44	±0.48
60-69	MEAN	2.48	2.07	5.7	4.88
	SD	±0.75	±0.41	±0.47	±0.3
70-79	MEAN	2.89	2.72	6	5.49
	SD	±0.68	±0.72	±0.26	±0.34

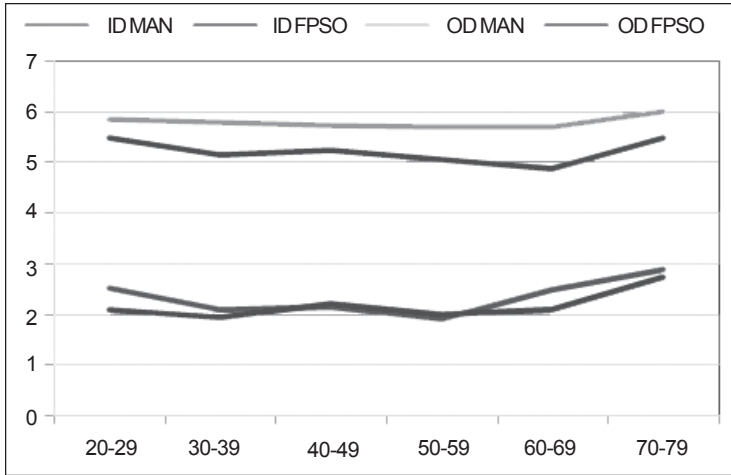


Figure 7: Line Graph of the ID and OD Measurements for the FPSO and Manual Measurement for C3

The line trends for the C3 ID measurements are very similar, Figure 7. Overall the ID and OD plots show that the FPSO obtains a very similar line trend to the manual measurements. Thus the Pearson correlation can be used to test the correlation between the ID and OD of the manual and FPSO measurements. The results of the Pearson correlation between the ID and OD measurements indicate a high degree correlation between the FPSO and the manual measurements.

The cortical thickness is another measurement that has been used to evaluate the accuracy of the measurements. The average CT measurements are presented in Table 8.

Table 8: Pearson Correlation between the ID and OD Measurement between the FPSOCFH and Manual Measurements

	C2	C3	C4
PSOCFHID	0.93	0.97	0.77
PSOCFHOD	0.82	0.67	0.83



Table 9: Comparison of the CT Measurements from FPSO with Manual Measurements

		C2-CT		C3-CT		C4-CT	
		MAN	FPSO	MAN	FPSO	MAN	FPSO
20-29	MEAN	4.37	4.37	4.02	4.02	3.32	3.41
	SD	±0.62	±0.38	±0.67	±0.63	±0.61	±0.48
30-39	MEAN	4.79	4.22	4.45	4.00	3.68	3.23
	SD	±0.63	±0.36	±0.44	±0.28	±0.65	±0.45
40-49	MEAN	4.76	4.15	4.35	3.76	3.59	3.05
	SD	±0.59	±0.07	±0.72	±0.09	±0.65	±0.10
50-59	MEAN	5.07	4.18	4.51	3.87	3.80	3.06
	SD	±0.53	±0.24	±0.52	±0.34	±0.59	±0.26
60-69	MEAN	4.32	3.50	3.80	3.28	3.22	2.82
	SD	±0.70	±0.31	±0.77	±0.33	±0.84	±0.34
70-79	MEAN	4.04	3.68	3.31	3.09	3.11	2.77
	SD	0.71	0.58	0.63	0.53	0.45	0.41

The CT measurement standard deviations using the FPSO are significantly lower than those for the manual measurements. The CT measurements in certain cases are the same as the manual measurements, thus providing further support to the accuracy of the FPSO measurements. The high manual CT measurement standard deviations may be attributed to the accuracy and consistency of the human eye in detecting the cortical outlines.

The above discussions have proven that the geometric measurements using the FPSO are sufficiently accurate if not better than the manual measurements. Table 9 presents the percentage accuracy between the FPSO measurements and the manual measurements. The percentage accuracy is higher than 80 % for all the measurements, which is quite high.

Table 10: Comparison of Percentage of Accuracy between the Manual Measurements and the Various Edge Detection Methods

Age	20 - 29.99	30 - 39.99	40 - 49.99	50 - 59.99	60 - 69.99	70 - 79.99
FPSO C2	99.98 %	88.09 %	87.14 %	82.53 %	81.03 %	91.09 %
FPSO C3	99.99 %	89.96 %	86.37 %	85.82 %	86.42 %	93.33 %
FPSO C4	97.20 %	87.86 %	85.07 %	80.56 %	87.55 %	89.23 %

## **Conclusion**

The use of the FPSO edge detection technique has been proven to be more sensitive in detecting the IC or weaker edges. The ID, OD and CT measurements for the FPSO measurements correlate very well with the manual measurements performed by doctors. In fact the standard deviation between the OD, ID and CT measurements are lower than those for the manual measurements, which indicates the accuracy and sensitivity of the FPSO method is sufficient to measure the cortical strength of the long bones.

## **Acknowledgments**

I would like to thank Dr Hanafi Ali for his assistance in understanding the radiograph images and Ms Shafaf Ibrahim for her considerable assistance. I would also like to thank Mr. Mohamad Norman Mohd Nordin for providing the digitized images.

## **References**

- [1] L. O'Donnell, 2001. *Semi-Automatic Medical Image Segmentation*. Department of Electrical Engineering and Computer Science, Massachusetts Institute of Technology. Thesis.
- [2] W. Zhao, *et al.*, 2006. Radon transform -based skull identification with multi-resolution. *Proceedings of the International Conference on Information Conference on Information Acquisition*, Shandong, China.
- [3] Noor Elaiza Abdul Khalid, *et al.*, 2007. CR images of metacarpel cortical edge detection-bone profile histogram approximation method, *Intelligent and Advanced Systems*, ICIAS 2007, pp. 702-708.
- [4] R. C. Gonzalez and R. E. Woods, 2002. *Digital Image Processing*. 2nd. s.l. : Addison Wesley.
- [5] Y. Becerikli and T. M. Karan, 2005. *A new fuzzy approach to edge detection*. Lecture Notes in Computer Science. Computational

Intelligence and Bioinspired Systems. s.l.: Springer Berlin / Heidelberg, pp. 943-951.

- [6] S. E. El-Khamy, I. A. Ghaleb and N. A. El-Yamany, 2002. *Minimum Entropy-Based Fuzzy Edge Detection*. XXVIIth General Assembly URSI GA.
- [7] M. Hanmandlu, J. See and S. Vasikarla, 2004. Fuzzy Edge Detector Using Entropy Optimization. *Proceedings of the International Conference on Technology: Coding and Computing*, pp. 665-670.
- [8] B. G. Kim and D. J. Park, 2002. Automatic Video Object Segmentation Based on New Edge Features, *International Conference on Signal Processing, Pattern Recognition and Applications*, pp. 488-492.
- [9] H. R. Tizhoosh, 2002. Fast Fuzzy Edge Detection. *North American Fuzzy Information Processing Society*, pp. 239-242.
- [10] K. Hirota and W. Pedrycz, 1999. Fuzzy Relational Compression. *IEEE Transactions on Systems, Man, and Cybernetic*, vol. 29.
- [11] J. See, M. Hanmandlu and S. Vasikarla, 2005. Fuzzy-based Parameterized Gaussian Edge Detector Using Global and Local Properties. *Proceedings of the International Conference on Information Technology: Coding and Computing*, pp. 101-106.
- [12] J. Kennedy and R. C. Eberhart, 1995. Particle swarm optimization. *Proceedings of IEEE International Conference on Neural Networks*. Piscataway, NJ, pp. 1942-1948.
- [13] A. S. Chernyavskiy, 2007. *Discrete attribute-based particle swarm optimization for robust parameter estimation*. Russia, Moscow, GraphiCon'2007.
- [14] M. Clerc, 2001. *Think Locally, Act Locally: The Way of Life of Cheap-PSO, an Adaptive PSO*. Technical report.

- [15] S. Das, A. Ajith and A. Konar, 2006. Spatial Information Based Image Segmentation Using a Modified Particle Swarm Optimization Algorithm. s.l. : IEEE Computer Society Washington, DC, USA, *Proceedings of the Sixth International Conference on Intelligent Systems Design and Applications (ISDA'06)*, vol. 02, pp. 438-444.
- [16] S. Saatchi and Hung, Chih-Cheng, 2007. *Swarm Intelligence and Image Segmentation*. Open Access Database [www.itechonline.com](http://www.itechonline.com). pp. 163-178.
- [17] S. Das, A. Ajith and S. K. Sark, 2006. A Hybrid Rough Set – Particle Swarm Algorithm for Image Pixel Classification. *HIS '06. Sixth International Conference on Hybrid Intelligent Systems*, pp. 26-26.
- [18] C. W. Lee, 2004. *The Determination of Bone Mineral Density of Local Malay Female And It's Correlation With Geometric Properties In The Evaluation of Skeletal Status*. s.l. : thesis, University Science of Malaysia.
- [19] Noor Elaiza Abdul Khalid, Mazani Manaf and Mohd Ezane Aziz, 2008. *Modified Fuzzy Heuristics Edge Detection – Tubular Bone Boundary Detection*. National Seminar of Fuzzy Theory and Application, Shah Alam.
- [20] M. Omran, 2004. *Particle Swarm Optimization Methods for Pattern Recognition and Image Processing*. PhD Thesis, University of Pretoria.
- [21] M. G. Omran, P. A. Engelbrecht and A. Salman, 2005. A Color Image Quantization Algorithm Based on Particle Swarm Optimization. *Informatica* 29, pp. 261-269.
- [22] J. Kennedy, 1997. The particle swarm: Social adaptation of knowledge. *IEEE International Conference on Evolutionary Computation*, pp. 303-308.

- [23] A. Carlisle and G. Dozier, 2000. Adapting Particle Swarm Optimization to Dynamic Environments. *Proceedings of the 2000 International Conference on Artificial Intelligence*, pp. 429-433.
- [24] V. D. Bergh and A. Engelbrecht, 2001. Effects of Swarm Size on Cooperative Particle Swarm Optimizers, *Proceedings of the Genetic and Evolutionary Computation Conference, GECCO 2001*, pp. 892-899.
- [25] P. Suganthan, 1999. Particle Swarm Optimiser with Neighborhood Operator, *Proceedings of the 1999 Congress on Evolutionary Computation*, pp. 1958-1962.

